

---

# Geodesic Distance Between Graphs: A Spectral Metric for Assessing the Stability of Graph Neural Networks

---

Soumen Sikder Shuvo   Ali Aghdai   Zhuo Feng  
Stevens Institute of Technology  
{sshuvo, aaghdaei, zhuo.feng}@stevens.edu

## Abstract

This paper presents a spectral framework for assessing the generalization and stability of Graph Neural Networks (GNNs) by introducing a Graph Geodesic Distance (GGD) metric. For two different graphs with the same number of nodes, our framework leverages a spectral graph matching procedure to find node correspondence so that the geodesic distance between them can be subsequently computed by solving a generalized eigenvalue problem associated with their Laplacian matrices. For graphs with different sizes, a resistance-based spectral graph coarsening scheme is introduced to reduce the size of the bigger graph while preserving the original spectral properties. We show that the proposed GGD metric can effectively quantify dissimilarities between two graphs by encapsulating their differences in key structural (spectral) properties, such as effective resistances between nodes, cuts, the mixing time of random walks, etc. Through extensive experiments comparing with the state-of-the-art metrics, such as the latest Tree-Mover’s Distance (TMD) metric, the proposed GGD metric shows significantly improved performance for stability evaluation of GNNs especially when only partial node features are available.

## 1 Introduction

In the era of big data, comparison and distinction between data points are important tasks. A graph is a specific type of data structure that represents the connections between a group of nodes or agents. Comparing two graphs often involves using a pairwise distance measure, where a small distance indicates a high structural similarity and vice versa. To understand the generalization between distribution shifts, it is important to use an appropriate measure of divergence between data distributions, both theoretically and experimentally [12]. Determining suitable distance metrics for non-Euclidean data entities, like graphs with or without node attributes, which are fundamental to many graph learning methods such as graph neural networks (GNNs), remains a significant challenge, even though distance metrics for data points in Euclidean space are readily available. The need to develop new analytical techniques that allow the visualization, comparison, and understanding of different graphs has led to a rich field of research study [25]. This study dives into the exploration of a novel framework for computing geometric distances between graphs, which can be immediately leveraged for many graph-based machine learning (ML) tasks, such as the stability evaluation of GNNs.

Many distance metrics for comparing graphs have previously been proposed [4]. Some of them are merely based on graph local structures [26, 56, 59, 18, 7], whereas others exploit both graph structural properties and node attributes [47, 37]. For example, the Graph Edit Distance (GED) has been proposed to measure the distance between graphs considering the number of changes needed to match one graph to another [45, 20, 30]; Distance metrics based on the graph kernel have also been investigated [47, 52], such as the Wasserstein Weisfeiler-Leman metric (WWL) [37] and the Gromov–Wasserstein metric [36], which allow computing graph distances based on

low-dimensional graph representations or optimal transport (OT) [49, 9], leading to the development of the state-of-the-art graph distance metric called Tree Mover’s Distance (TMD) [11].

However, the existing graph distance metrics have distinct limitations. For example, the GED metric can capture local node or edge changes but struggles with global perturbations [45, 20, 30]; the WWL and TMD metrics heavily rely on node features (attributes) for calculating the distance between graphs, leading to degraded performance when only partial node features are available [43, 10].

To address the limitations of prior methods, we propose a Graph Geodesic Distance (GGD) metric that can be computed through the following steps: for two graphs of the same size (with  $n$  nodes), (1) a spectral graph matching procedure is exploited for finding the node correspondence between two graphs, and (2) a geodesic distance metric is defined on the cone of  $n \times n$  modified graph Laplacians that can be regarded as a Riemannian manifold [32]. For graphs of different sizes, we introduce a resistance-based spectral graph coarsening scheme to transform the larger graph into a smaller one suitable for the GGD evaluation. We show that the proposed GGD metric can theoretically capture key structural (spectral) dissimilarities between two graphs, such as mismatches in Laplacian eigenvalues/eigenvectors, cuts, effective-resistance distances, etc.

One distinct advantage of the proposed GGD metric is its capability to compute distances between graphs based on their spectral (structural) properties, while including node feature information into our framework can further improve the accuracy. Therefore, GGD is suitable for analyzing many real-world graphs that may only have partial or even no node features. Moreover, the proposed framework for computing GGDs is more computationally efficient than existing OT-based metrics, such as the TMD metric. Our preliminary results show that the GGD metric has a better correlation with established GNN output compared to the state-of-the-art TMD metric [11]. It also allows us to achieve up to 10% accuracy gain and  $9\times$  runtime speedup in graph classification tasks than TMD.

## 2 Existing Graph Distance Metrics

**Graph Edit Distance (GED)** For non-attributed graph data, a common and simple distance metric is GED. [45, 20]. Given a set of graph edit operations, also known as elementary graph operations, the GED between two graphs  $G_1$  and  $G_2$ , written as  $\text{GED}(G_1, G_2)$ , can be defined as:

$$\text{GED}(G_1, G_2) = \min_{(e_1, \dots, e_k) \in \mathcal{P}(G_1, G_2)} \sum_{i=1}^k c(e_i) \quad (1)$$

where  $\mathcal{P}(G_1, G_2)$  denotes the set of edit operations transforming  $G_1$  into a graph isomorphism of  $G_2$ ,  $c(e_i)$  is the cost of edit operation  $e_i$ . The set of elementary graph edit operators typically includes node insertion, node deletion, node substitution, edge insertion, edge deletion, and edge substitution.

**Tree Mover’s Distance (TMD)** TMD is a pseudometric for measuring distances between simple graphs, extending the concept of WWL to multisets of tree structures [11]. By progressively adding neighboring nodes to the previous node at each level, we obtain the computation tree of a node. These tree structures are crucial in graph analysis [54, 40] and graph kernels [42, 47]. TMD uses hierarchical optimal transport (HOT) to analyze these computational trees from input graphs. For a graph  $G = (V, E)$  with node features  $f_v \in \mathbb{R}^s$  for node  $v \in V$ , let  $T_v^1 = v$ , and  $T_v^L$  be the depth- $L$  computation tree of node  $v$ . The multiset of these trees for  $G$  is  $T_G^L = \{T_v^L\}_{v \in V}$ . The number and shape of trees must match to calculate optimal transport between two multisets of trees. If multisets are uneven, they are augmented with blank nodes. For multisets  $T_p$  and  $T_q$ , the augmenting function  $\sigma$  adds blank trees to equalize their sizes. A blank tree  $T_0$  has a single node with a zero vector feature  $0_p \in \mathbb{R}^s$ :

$$\sigma : (T_p, T_q) \rightarrow (T_p \cup T_0^{\max(|T_q| - |T_p|, 0)}, T_q \cup T_0^{\max(|T_p| - |T_q|, 0)}) \quad (2)$$

Let  $X = \{x_i\}_{i=1}^k$  and  $Y = \{y_j\}_{j=1}^k$  be two data multisets and  $C \in \mathbb{R}^{k \times k}$  be the transportation cost for each data pair:  $C_{ij} = d(x_i, y_j)$ , where  $d$  is the distance between  $x_i$  and  $y_j$ . The unnormalized Optimal Transport between  $X$  and  $Y$  can be defined as:

$$\text{OT}_d(X, Y) := \min_{\gamma \in \Gamma(X, Y)} \langle C, \gamma \rangle \quad \Gamma(X, Y) = \{\gamma \in \mathbb{R}_+^{m \times m} \mid \gamma \mathbb{1}_m = \gamma^\top \mathbb{1}_m = \mathbb{1}_m\} \quad (3)$$

Here  $\Gamma$  is the set of transportation plans that satisfies the flow constrain  $\gamma \mathbb{1}_m = \gamma^\top \mathbb{1}_m = \mathbb{1}_m$  [11].

The distance between two trees  $T_p$  and  $T_q$  with roots  $r_p$  and  $r_q$  is defined recursively:

$$\text{TD}_w(T_p, T_q) := \begin{cases} \|f_{r_p} - f_{r_q}\| + w(L) \cdot \text{OT}_{\text{TD}_w}(\sigma(T_{r_p}, T_{r_q})) & \text{if } L > 1 \\ \|f_{r_p} - f_{r_q}\| & \text{otherwise} \end{cases} \quad (4)$$

where  $L$  is the maximum depth of  $T_p$  and  $T_q$ , and  $w$  is a depth-dependent weighting function. Subsequently, the concept of distance from individual trees is enlarged to entire graphs. For graphs  $G_1$  and  $G_2$ , with multisets  $\mathbf{T}_{G_1}^L$  and  $\mathbf{T}_{G_2}^L$  of depth- $L$  computation trees, the Tree Mover’s Distance is:

$$\text{TMD}_w^L(G_1, G_2) = \text{OT}_{\text{TD}_w}(\sigma(\mathbf{T}_{G_1}^L, \mathbf{T}_{G_2}^L)) \quad (5)$$

### 3 GGD: A Geodesic Distance Metric for Graphs

**Laplacian matrices on the Riemannian manifold** To overcome the limitations of the previous OT-based graph distance metrics [11], we aim to develop a new pseudometric that can effectively encapsulate topological differences between graphs. One way to represent a simple graph is through its Laplacian matrix, which is a Symmetric Positive Semidefinite matrix. Adding a small positive value to each diagonal element will allow us to transform the original Laplacian matrix into a Symmetric Positive Definite (SPD) one, which is called the **modified Laplacian matrix** in this work. Then we can consider the cone of such modified Laplacian matrices as a natural Riemannian manifold [32], where each modified Laplacian has the same dimensions (same number of rows/columns) and can be regarded as a data point on the Riemannian manifold [51, 41]. In the last, the geodesic distance between two graphs can be defined as the shortest path distance on the Riemannian manifold if their node correspondence is known in advance. This approach is more appropriate than directly comparing the graphs in the Euclidean space [32, 13, 27]. We will later show (Section 4.3) that such a geodesic distance metric can effectively capture structural (spectral) mismatches between graphs.

**A spectral framework for computing GGDs** Before computing GGDs, it is necessary to establish the node-to-node correspondence between two graphs. This can be achieved by leveraging existing graph-matching techniques [33, 15, 8]. In this work, we will leverage a recent spectral graph matching framework that has been shown to recover accurate matching with high probability [16].

The proposed GGD metric can be computed in the following two phases. **Phase 1** consists of a spectral graph matching step, using combinatorial optimization with the eigenvalues/eigenvectors of the graph adjacency matrices to identify the approximate node-to-node correspondence. **Phase 2** computes the GGD between the modified Laplacian matrices of the matched graphs by exploiting generalized eigenvalues. The proposed GGD metric differs from previous OT-based graph distance metrics in its ability to accurately represent structural discrepancies between graphs, enabling us to uncover the topological variations between them more effectively. Since only the graph Laplacian (adjacency) matrix is required to calculate the GGD, our metric can even work effectively for graphs without node feature information.

**A motivating example** Let’s consider a simple graph  $G_1$ , characterized by an almost ring-like topology, as shown in Figure 1. We also create two other graphs  $G_2$  and  $G_3$  by inserting an extra edge into  $G_1$  in different ways. Note that the additional edge in  $G_3$  will have a greater impact on  $G_1$ ’s global structure since it connects two further nodes.

Table 1: Distance between graphs with simple perturbation

We compute the normalized distances (the largest distance always equals one) between the aforementioned three graphs using different metrics (GED, TMD, and GGD) and report the results in Table 1. As observed,  $G_2$  and  $G_3$  have distances similar to  $G_1$  when the TMD metric is adopted without using node features (NFs). On the other hand, the TMD metric can produce similar results as the proposed GGD metric when node features are fully utilized. Not

Graph Pairs	Distance Metrics (Normalized)			
	GGD	TMD with NF, L = 4	TMD without NF, L = 4	GED
$G_1, G_2$	0.623	0.689	0.970	1
$G_1, G_3$	0.855	0.711	1	1
$G_2, G_3$	1	1	0.333	1

surprisingly, the GED always produces the same distances since only one edge has been added. The above results imply that the GED and TMD (without using NFs) metrics may not properly capture the dissimilarities in the structural (spectral) properties of the graphs.

## 4 Computing GGDs Between Graphs of the Same Size

### 4.1 Phase 1: Spectral Graph Matching for Finding Node Correspondence

Computing the GGD metric between two input graphs requires solving a graph matching problem in advance. Graph matching techniques can be used to establish node-to-node correspondence by seeking a bijection between node sets to maximize the alignment of edge sets [33, 15, 8]. This combinatorial optimization problem can be cast into a Quadratic Assignment Problem, which is NP-hard to solve or approximate [16, 53].

In this study, we will exploit a spectral graph matching method called GRAMPA (**GRA**ph **M**atching by **P**airwise eigen-**A**lignments) [16] to find the approximate node correspondence between two graphs. GRAMPA starts with comparing the eigenvectors of the adjacency matrices of the input graphs. Instead of comparing only the eigenvectors responding to the largest eigenvalues, it considers all pairs of eigenvectors/eigenvalues to generate a similarity matrix. This similarity matrix can be constructed by summing up the outer products of eigenvector pairs, weighted by a Cauchy kernel [16]. Subsequently, a rounding procedure will be performed to determine the optimal match between nodes employing the similarity matrix.

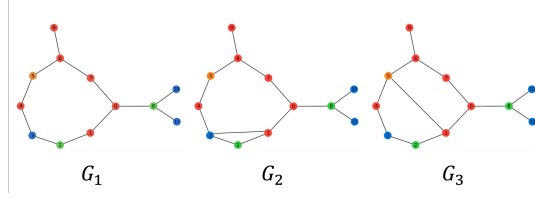


Figure 1: Graphs with simple perturbations

**Definition 4.1** (Similarity Matrix). Let  $G_1$  and  $G_2$  be two undirected graphs with  $n$  nodes, and let their weighted adjacency matrices be  $A_1$  and  $A_2$ , respectively. The spectral decompositions of  $A_1$  and  $A_2$  are expressed as follows:  $A_1 = \sum_{i=1}^n \zeta_i u_i u_i^\top$  and  $A_2 = \sum_{j=1}^n \mu_j v_j v_j^\top$ , where the eigenvalues are ordered such that  $\zeta_1 \geq \dots \geq \zeta_n$  and  $\mu_1 \geq \dots \geq \mu_n$ . The similarity matrix  $\hat{X} \in \mathbb{R}^{n \times n}$  is defined as:

$$\hat{X} = \sum_{i,j=1}^n w(\zeta_i, \mu_j) \cdot u_i u_i^\top \mathbf{J} v_j v_j^\top, \quad \text{where } w(x, y) = \frac{1}{(x - y)^2 + \eta^2} \quad (6)$$

Here,  $\mathbf{J} \in \mathbb{R}^{n \times n}$  denotes an all-one matrix and  $w$  is the Cauchy kernel of bandwidth  $\eta$ .

The permutation estimate matrix  $\hat{\pi}$  can be obtained by rounding  $\hat{X}$ , typically achieved by solving the Linear Assignment Problem (LAP):

$$\hat{\pi} = \operatorname{argmax} \sum_{i=1}^n \hat{X}_{i, \pi(i)} \quad (7)$$

This LAP can be solved efficiently using the Hungarian Algorithm [16, 29], where:

$$\hat{\pi}(i) = \operatorname{argmax}_j \hat{X}_{ij}. \quad (8)$$

**Lemma 4.1** (Graph Matching Recovery). *Given symmetric matrices  $A$ ,  $B$  and  $Z$  from the Gaussian Wigner model, where  $B_{\pi^*} = A + \sigma Z$ , there exist constants  $c, c' > 0$  such that if  $1/n^{0.1} \leq \eta \leq c/\log n$  and  $\sigma \leq c'\eta$ , then with probability at least  $1 - n^{-4}$ , GRAMPA Algorithm correctly recovers the permutation matrix  $\pi^*$  from the Similarity matrix  $\hat{X}$  [16]. Its proof can be found in the supporting documents A.2.*

Once  $\hat{\pi}$  is obtained, the best-matched mirrors of the input graphs are:

$$\text{Best Match to } B = \hat{\pi} \cdot A \cdot \hat{\pi}^\top, \quad \text{Best Match to } A = \hat{\pi}^\top \cdot B \cdot \hat{\pi} \quad (9)$$

In practice, the graph matching performance is not too sensitive to the choice of tuning parameter  $\eta$ . For small-sized graphs, such as the MUTAG dataset[38], setting  $\eta = 0.5$  yields satisfactory results in matching. In Appendix A.3, the effect of  $\eta$  for computing GGDs has been comprehensively analyzed.

## 4.2 Phase 2: Computing Geodesic Distances Between Graph Laplacians

The GGD metric can be formally defined as the infimum length of geodesics connecting two data points in the Riemannian manifold formed by the cone of the modified graph Laplacian matrices [32]. This distance metric can be imagined as a matrix representation of the geometric distance  $|\log(a/b)|$  between two positive numbers  $a, b$  [3, 46, 39].

**Definition 4.2** (Graph Geodesic Distance). Let  $\mathcal{L}_1$  and  $\mathcal{L}_2 \in \mathbb{S}_{++}^n$  denote two modified Laplacian matrices corresponding to two matched graphs  $G_1$  and  $G_2$  both having  $n$  nodes, then their Graph Geodesic Distance denoted by  $GGD(G_1, G_2) : \mathbb{S}_{++}^n \times \mathbb{S}_{++}^n \rightarrow \mathbb{R}_+$ , is defined as:

$$GGD(G_1, G_2) = \left[ \sum_{i=1}^n \log^2(\lambda_i(\mathcal{L}_1^{-1}\mathcal{L}_2)) \right]^{1/2} \quad (10)$$

where  $\lambda_i$  are the generalized eigenvalues computed with the matrix pencil  $(\mathcal{L}_1, \mathcal{L}_2)$ .

## 4.3 Connection between GGD and Graphs' Structural Mismatches

For two graphs  $G_1$  and  $G_2$  that share the same node set  $V$  (node correspondence is known in advance), let  $L_1$  and  $L_2$  be their respective Laplacian matrices. Consider a node subset denoted by  $S$  and its complement denoted by  $S'$ . We assign each node in  $S$  a value of 1, and each node in  $S'$  a value of 0. Then the node set  $S$  can be defined as:

$$S \stackrel{\text{def}}{=} \{v \in V : x(v) = 1\}$$

The graph cut for node subset  $S$ , corresponding to the number of edges crossing  $S$  and  $S'$  in graph  $G_1$  can be computed by:

$$\text{cut}_{G_1}(S, S') = x^T L_1 x$$

As illustrated in Figure 2, the node subset  $S$  has six edges crossing the boundary in  $G_1$  but only two in  $G_2$ . This cut mismatch can be related to the generalized eigenvalue of the matrix pencil  $(L_1, L_2)$  using the Generalized Courant-Fischer Minimax Theorem [23, 17].

**Lemma 4.2** (The Generalized Courant-Fischer Minimax Theorem). *Given two Laplacian matrices  $L_1, L_2 \in \mathbb{R}^{n \times n}$  such that  $\text{null}(L_2) \subseteq \text{null}(L_1)$ , the  $k$ -th largest generalized eigenvalue of  $L_1$  and  $L_2$  can be computed as follows for  $1 \leq k \leq \text{rank}(L_2)$ :*

$$\lambda_k = \min_{\substack{\dim(U)=k \\ U \perp \text{null}(L_2)}} \max_{x \in U} \frac{x^T L_1 x}{x^T L_2 x} \quad (11)$$

This theorem allows us to find the upper bound of the maximum cut mismatch between two graphs by computing the most dominant generalized eigenvalue via the following optimization problem [17]:

$$\lambda_{\max} = \max_{\substack{|x| \neq 0 \\ x^T \mathbf{1} = 0}} \frac{x^T L_1 x}{x^T L_2 x} \geq \max_{\substack{|x| \neq 0 \\ x(v) \in \{0,1\}}} \frac{x^T L_1 x}{x^T L_2 x} = \max \frac{\text{cut}_{G_1}(S, S')}{\text{cut}_{G_2}(S, S')} \quad (12)$$

Based on (12), we can infer that the dominant generalized eigenvalue is closely related to the most significant graph cut mismatch between graphs  $G_1$  and  $G_2$ . As a result,  $\lambda_{\max} = \lambda_1$  connects to the upper bound of the cut mismatch between graphs  $G_1$  and  $G_2$ , whereas  $\lambda_{\min} = \lambda_n$  connects to the upper bound of the cut mismatch between graphs  $G_2$  and  $G_1$ . Similarly, the second-largest (smallest) eigenvalues correspond to the next most significant cut mismatches. It is also obvious that the generalized eigenvalues close to 1 will correspond to the minimum cut mismatches between two graphs.

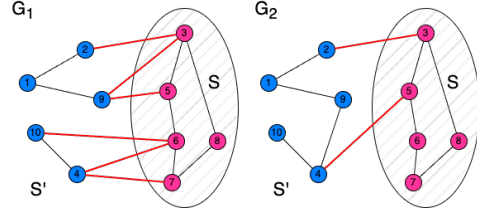


Figure 2: The cut mismatch (for the node set  $S$ ) between two simple graphs is  $\frac{6}{2} = 3$

## 5 Computing GGDs for Graphs with Different Sizes

**Submatrix selection methods** To calculate geodesic distances between SPD matrices of different sizes, prior studies have proposed a submatrix adaptation method [32]. In this approach, a principle submatrix with the same size as the smaller matrix is obtained from the larger matrix [57], and subsequently used to calculate the GGD. Furthermore, this method can be extended to project the smaller matrix into a larger one with the same size as the larger matrix [32]. While these methods are efficient for handling SPD matrices, for our application taking the submatrix of the modified Laplacian can lose important nodes/edges, compromising critical graph structural properties.

**Graph coarsening methods** In this work, we will leverage spectral graph coarsening to address the issue. Spectral graph coarsening is a widely adopted process [34, 1] for reducing graph sizes while preserving key spectral (structural) properties, such as the Laplacian eigenvalues/eigenvectors. Recent spectral graph coarsening methods aim to decompose an input graph into many distinct node clusters, so that a reduced graph can be formed by treating each node cluster as a new node, with a goal of assuring that the reduced graph will approximately retain the original graph’s structure [34, 24, 1]. Therefore, when computing GGDs for graphs of different sizes, we can first adopt spectral graph coarsening to transform the bigger graph into a smaller one, so that our framework in Section 4 can be subsequently utilized. However, existing state-of-the-art graph coarsening methods do not allow us to precisely control the size of the reduced graphs.

### 5.1 Our Approach: Spectral Graph Coarsening by Effective Resistances

In this work, we introduce a spectral graph coarsening method using effective-resistance clustering [1]. Our approach starts with estimating the effective resistances of all edges in the original graph. We can also incorporate the difference between node feature (if available) vectors as an additional parameter. In the graph coarsening phase, our method will rank edges according to their resistance distances and only the top few edges with the smallest resistances will be coarsened into new nodes. This approach enables precise control over the size of the reduced graphs while preserving crucial structural properties, such as the eigenvalues/eigenvectors of the adjacency matrices, which are essential for the subsequent spectral graph matching step (Phase 1 in Section 4.1).

Consider a connected, weighted, undirected graph  $G = (V, E, w)$  with  $|V| = n$ . The effective resistance between nodes  $(p, q) \in V$  plays a crucial role in various graph analysis tasks including spectral sparsification algorithms [48]. The effective resistance distances can be accurately computed using the equation:

$$R_{eff}(p, q) = \sum_{i=2}^n \frac{w_{p,q}(u_i^\top b_{pq})^2}{\sigma_i}, \quad (13)$$

where  $b_p \in \mathbb{R}^n$  denote the standard basis vector with all zero entries except for the  $p$ -th entry being 1, and  $b_{pq} = b_p - b_q$ .  $u_i \in \mathbb{R}^n$  for  $i = 1, \dots, n$  denote the unit-length, mutually-orthogonal eigenvectors corresponding to Laplacian eigenvalues  $\sigma_i$  for  $i = 1, \dots, n$ .

**Scalable estimation of effective resistances** To address the computational complexity associated with directly computing eigenvalues and eigenvectors required for estimating edge effective resistances, we leverage a scalable framework for approximating the eigenvectors of the graph Laplacian matrix using the Krylov subspace [44]. Let  $A$  denote the adjacency matrix of graph  $G$ , consider its order- $m$  Krylov subspace  $\mathbf{K}_m(A, x)$  that is a vector space spanned by the vectors computed through power iterations  $x, Ax, A^2x, \dots, A^{m-1}x$  [31]. By enforcing orthogonality among the above vectors in the Krylov subspace, a new set of mutually orthogonal vectors of unit lengths can be constructed for approximating the original Laplacian eigenvectors in 13, which are denoted as  $\tilde{u}_1, \tilde{u}_2, \dots, \tilde{u}_m$ . To estimate the effective resistance between two nodes  $p$  and  $q$ , we can exploit the approximated eigenvectors:

$$R_{eff}(p, q) \approx \sum_{i=1}^m \frac{w_{p,q}(\tilde{u}_i^\top b_{pq})^2}{\tilde{u}_i^\top L \tilde{u}_i}, \quad (14)$$

where  $\tilde{u}_i$  represents the approximated eigenvector corresponding to the  $i$ -th eigenvalue of  $L$ .

**Graph coarsening with node features** In order to account for the variation in node features along with edge resistive distance, we can use the following modified effective resistance formulation:

$$R_{eff}^*(p, q) = R_{eff}(p, q) + \alpha \|f_p - f_q\| \quad (15)$$

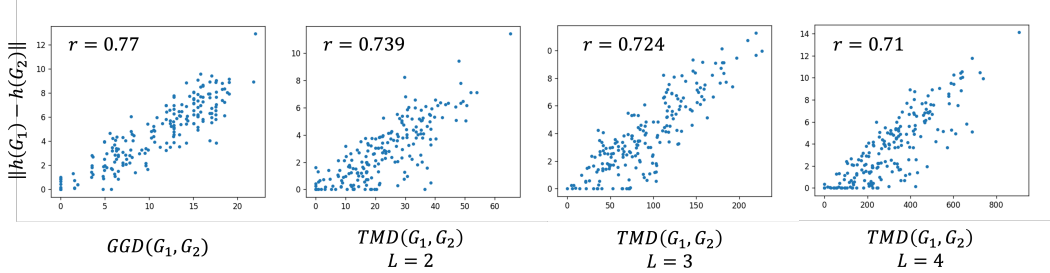


Figure 3: Correlation between graph distance metrics and GNN’s outputs

where  $f_p$  and  $f_q$  are node feature vectors of nodes  $p$  and  $q$ , respectively, while  $\alpha$  is a weighting factor that determines the effect of node feature information in the graph coarsening process.

## 6 GGD as a Distance Metric

Assuming that the graph matching problem can always find the exact correspondence between nodes, we prove that the GGD metric between any two (nonempty) graphs is a pseudometric that satisfies the following conditions:

- The distance between a graph and itself or between two isomorphic graphs is zero:  $GGD(G, G) = 0$ .
- (Positivity) The distance between two distinct graphs is positive:  $GGD(G_1, G_2) > 0$ .
- (Symmetry) The distance between  $G_1$  and  $G_2$  is the same of the one between  $G_2$  and  $G_1$ :  $GGD(G_1, G_2) = GGD(G_2, G_1)$ .
- The triangle inequality:  $GGD(G_1, G_3) \leq GGD(G_1, G_2) + GGD(G_2, G_3)$ .

Detailed proofs of the above four properties are provided in Appendix A.1.

## 7 Experiments

### 7.1 Stability Analysis of GNNS

To analyze the stability of GNN models [6, 21, 14], we conducted multiple experiments with the GGD and TMD metrics. GNNs typically operate by a message-passing mechanism [22], where at each layer, nodes send their feature representations to their neighbors. The feature representation of each node is initialized to its original features and is updated by repeatedly aggregating incoming messages from neighbors. In our experiment, we relate GGD to the Graph Isomorphism Networks (GIN) [55], one of the most widely applied and powerful GNNs, utilizing the MUTAG dataset [38] as our reference graph dataset. The objective is to analyze the relationship between the input distance  $GGD(G_1, G_2)$  and the distance between the output GIN vectors,  $\|h(G_1) - h(G_2)\|$  for randomly selected pairs of graphs. The result is illustrated in Figure 3.

We observe a strong correlation between GGD and the output distance, as indicated by a high Pearson correlation coefficient. This finding implies the effectiveness of the proposed GGD metric for analyzing the stability of GNN models [11]. To compare GGD with existing metrics, we repeat this experiment using TMD without considering node attributes (features). As shown in Figure 3, GGD demonstrates a better correlation with GIN outputs than the TMD metric across different levels. These findings indicate that when dealing with graphs without node features, GGD should be adopted for the stability analysis of graph learning models.

### 7.2 Graph Classification

We evaluate whether the GGD metric aligns with graph labels in graph classification tasks using datasets from TUDatasets [38]. We employ a Support Vector Classifier (SVC) ( $C = 1$ ) with an indefinite kernel  $e^{-\gamma * GGD(G_1, G_2)}$ , which can be viewed as a noisy observation of the true positive

Table 2: Classification accuracies for various models on graph datasets

Dataset	Accuracy in percentage			
	MUTAG	PC-3H	SW-620H	BZR
GGD	$86 \pm 7.5$	<b>78.34</b>	<b><math>77.6 \pm 3.5</math></b>	<b>83.23</b>
TMD, L = 2	$76 \pm 5.3$			
TMD, L = 3	$77 \pm 5.2$	71.24	$70.2 \pm 2.3$	73.43
TMD, L = 4	$78.2 \pm 6$	71.37	$70.8 \pm 2.3$	73.96
TMD, L = 5		71.89	$71.2 \pm 1.88$	75.13
GCN[28]	$77 \pm 3.8$	70.56	69.4	72.56
GIN[55]	$82.6 \pm 4.6$	<u>75.34</u>	<u>73.4</u>	<u>77.09</u>
WWL[50]	$72.4 \pm 2.6$	65.46	68.34	73.59
WL Subtree[47]	$76 \pm 6.3$	68.43	70.56	N/A
FGH[49]	<b><math>88.33 \pm 5.6</math></b>	61.77	59.3	53.66

semidefinite kernel [35]. The parameter  $\gamma$  is selected through cross-validation from the set  $\{0.01, 0.05, 0.1\}$ . For comparative analysis with existing methods, we include graph kernels based on graph subtrees: the WL subtree kernel [47]; and two widely adopted GNNs: graph isomorphism network (GIN) [55] and graph convolutional networks (GCN) [28].

Table 2 presents the mean and standard deviation over five independent trials with a 90%-10% train-test split. For most cases, GGD consistently outperforms the performance of state-of-the-art GNNs, graph kernels, and metrics when node attributes are missing. Additionally, we observe that GGD allows us to obtain better results for larger datasets than smaller ones.

### 7.3 Runtime Complexity Analysis and Comparison

When comparing various graph distance metrics, a primary consideration is their computational complexity. Conventional approaches usually require intricate computations that frequently have cubic time or higher complexities. For our problem, the spectral graph matching step requires the eigenvalue decomposition of adjacency matrices and solving the linear

assignment problem (LAP). Eigenvalue decomposition of an  $n \times n$  matrix has a complexity of  $O(n^3)$  [5, 2], while solving the LAP using the Hungarian algorithm also has a runtime complexity of  $O(n^3)$ . Similarly, calculating the generalized eigenvalue of two SPD matrices entails a cubic complexity. Consequently, the overall complexity of GGD calculation is  $O(n^3)$ . On the other hand, TMD is an OT-based distance metric with a complexity of  $O(n^3 \log(n))$  [11, 19]. Therefore, GGD exhibits slightly better (lower) runtime complexity than the TMD metric.

To evaluate runtime performance, we conduct extensive experiments to compare the runtime of computing TMD at various levels with GGD on both small graphs (MUTAG, BZR) and large graphs (PC-3H, SW-620H) collected from the TUDataset [38]. Table 3 presents the average runtime (in seconds) for computing 100 distances between different graphs obtained by repeating the experiment five times. The results demonstrate that GGD consistently outperforms TMD in terms of runtime across all datasets and scenarios, particularly when dealing with larger graphs that contain more nodes. The TMD metric computation usually requires more levels to effectively capture the entire graph structure. In such cases, GGD exhibits runtime performance approximately 6 – 9 times faster than of TMD. Hence, we conclude that GGD is significantly more computationally efficient than TMD, especially when working with large graphs. More details about our experimental setup can be found in Appendix A.4.

Table 3: Runtime comparison for different distance metrics on various datasets.

	MUTAG	PC-3H	SW-620H	BZR
GGD	<b>4.87 s</b>	<b>31.89 s</b>	<b>45.37 s</b>	<b>5.80 s</b>
TMD, L = 3	5.30 s	88.6 s	98.7 s	7.22 s
TMD, L = 4	7.89 s	112 s	134.38 s	10.34 s
TMD, L = 6	11.27 s	273 s	288 s	14.98 s



## 7.4 Partial Node Features

Cutting-edge graph distance metrics like TMD, rely on node attributes to compute the dissimilarity between graphs, resulting in more accurate outcomes when all attributes are available. However, acquiring datasets with complete node attributes is often unattainable in real-world scenarios, leading to situations where certain features are partially missing. In such scenarios when only partial node features are available, we compare TMD with GGD to better understand their differences. Table 4 shows that the TMD metric outperforms GGD at various levels when node features are fully accessible. However, when node features are randomly removed from the MUTAG dataset, the accuracy of TMD degrades substantially.

Distance Metric	Node Features Missing in Percentage				
	0%	20%	50%	80%	100%
TMD, L = 3	<b>0.84</b>	<b>0.78</b>	0.72	0.63	0.61
TMD, L = 4	0.81	0.77	0.62	0.58	0.57
TMD, L = 5	0.80	0.75	0.65	0.58	0.53
GGD	0.78	<b>0.78</b>	<b>0.77</b>	<b>0.77</b>	<b>0.77</b>

Table 4: Comparison of Correlation with GNN outputs and distance metrics with Partial Node Features

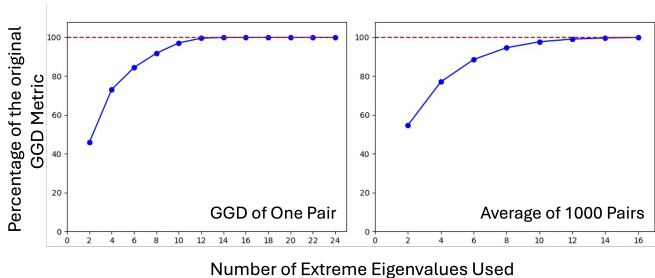


Figure 4: Percentage of the original GGD using numbers of extreme Eigenvalues

## 7.5 GGD Approximation using Extreme Eigenvalues

The largest or smallest eigenvalues correspond to the most dominant mismatches in graph cuts and effective resistance distances, contributing most to the total GGD value. Similarly, the

Table 5: Performance of GGD using Extreme Eigenvalues only

Task	Number of Extreme Eigenvalues		
	2	4	All
Correlation with GNN	0.74	0.76	0.77
Classification Accuracy	81.50 ± 6.85	83.87 ± 7.56	86.00 ± 7.5

second largest and smallest eigenvalues correspond to the next significant mismatched cuts. In our experiment, we obtain approximate GGDs using a few extreme eigenvalue pairs and compare them with the ground truth. Figure 4 illustrates the relative accuracy of the approximate GGDs, in which we observe that the top four pairs of extreme eigenvalues contribute 80% of the total GGD values. In addition, we conduct the SVC classification task and GNN correlation study using GGD with only 2 and 4 extreme eigenvalue pairs, respectively and present the associated findings in Table 5.

## 8 Conclusion

In this work, we introduce Graph Geodesic Distance (GGD), a novel spectral graph distance metric based on graph matching and the infimum on a Riemannian manifold. GGD captures the essential structural mismatches of graphs vital for graph classification tasks. Additionally, we show that GGD can serve as an effective metric for analyzing the stability of GNN models and graph classification tasks, achieving superior performance when only partial node features are available.

## References

- [1] Ali Aghdaei and Zhuo Feng. Hyperref: Spectral hypergraph coarsening by effective-resistance clustering. In *Proceedings of the 41st IEEE/ACM International Conference on Computer-Aided Design*, pages 1–9, 2022.
- [2] Rémi André, Tual Trainini, Xavier Luciani, and Eric Moreau. A fast algorithm for joint eigenvalue decomposition of real matrices. In *2015 23rd European Signal Processing Conference (EUSIPCO)*, pages 1316–1320, 2015. doi: 10.1109/EUSIPCO.2015.7362597.
- [3] Silvere Bonnabel and Rodolphe Sepulchre. Riemannian metric and geometric mean for positive semidefinite matrices of fixed rank. *SIAM Journal on Matrix Analysis and Applications*, 31(3): 1055–1070, 2010.
- [4] Karsten Borgwardt, Elisabetta Ghisu, Felipe Llinares-López, Leslie O’Bray, and Bastian Rieck. Graph kernels: State-of-the-art and future challenges. *Foundations and Trends® in Machine Learning*, 13(5-6):531–712, 2020. ISSN 1935-8237.
- [5] A. Borodin and I. Munro. *The Computational Complexity of Algebraic and Numeric Problems*. Elsevier Computer Science Library, Theory of Computation Series. American Elsevier Publishing Company, 1975. ISBN 9780608163741.
- [6] Michael M Bronstein, Joan Bruna, Yann LeCun, Arthur Szlam, and Pierre Vandergheynst. Geometric deep learning: going beyond euclidean data. *IEEE Signal Processing Magazine*, 34(4):18–42, 2017.
- [7] Horst Bunke and Kim Shearer. A graph distance metric based on the maximal common subgraph. *Pattern recognition letters*, 19(3-4):255–259, 1998.
- [8] Tibério S Caetano, Julian J McAuley, Li Cheng, Quoc V Le, and Alex J Smola. Learning graph matching. *IEEE transactions on pattern analysis and machine intelligence*, 31(6):1048–1058, 2009.
- [9] Laetitia Chapel, Mokhtar Z Alaya, and Gilles Gasso. Partial optimal transport with applications on positive-unlabeled learning. *Advances in Neural Information Processing Systems*, 33:2903–2913, 2020.
- [10] Xu Chen, Siheng Chen, Jiangchao Yao, Huangjie Zheng, Ya Zhang, and Ivor W Tsang. Learning on attribute-missing graphs. *IEEE transactions on pattern analysis and machine intelligence*, 44(2):740–757, 2022.
- [11] Ching-Yao Chuang and Stefanie Jegelka. Tree mover’s distance: Bridging graph metrics and stability of graph neural networks. *Advances in Neural Information Processing Systems*, 35: 2944–2957, 2022.
- [12] Ching-Yao Chuang, Antonio Torralba, and Stefanie Jegelka. Estimating generalization under distribution shifts via domain-invariant representations. *International conference on machine learning*, 2020.
- [13] Keenan Crane, Marco Livesu, Enrico Puppo, and Yipeng Qin. A survey of algorithms for geodesic paths and distances. *arXiv preprint arXiv:2007.10430*, 2020.
- [14] David K Duvenaud, Dougal Maclaurin, Jorge Iparraguirre, Rafael Bombarell, Timothy Hirzel, Alán Aspuru-Guzik, and Ryan P Adams. Convolutional networks on graphs for learning molecular fingerprints. *Advances in neural information processing systems*, 28, 2015.
- [15] Frank Emmert-Streib, Matthias Dehmer, and Yongtang Shi. Fifty years of graph matching, network alignment and network comparison. *Information sciences*, 346:180–197, 2016.
- [16] Zhou Fan, Cheng Mao, Yihong Wu, and Jiaming Xu. Spectral graph matching and regularized quadratic relaxations: Algorithm and theory. In *International conference on machine learning*, pages 2985–2995. PMLR, 2020.
- [17] Zhuo Feng. Grass: Graph spectral sparsification leveraging scalable spectral perturbation analysis. *IEEE Transactions on Computer-Aided Design of Integrated Circuits and Systems*, 39(12):4944–4957, 2020.
- [18] Mirtha-Lina Fernández and Gabriel Valiente. A graph distance metric combining maximum common subgraph and minimum common supergraph. *Pattern Recognition Letters*, 22(6-7): 753–758, 2001.

- [19] Rémi Flamary, Nicolas Courty, Alexandre Gramfort, Mokhtar Z Alaya, Aurélie Boisbunon, Stanislas Chambon, Laetitia Chapel, Adrien Corenflos, Kilian Fatras, Nemo Fournier, et al. Pot: Python optimal transport. *Journal of Machine Learning Research*, 22(78):1–8, 2021.
- [20] Xinbo Gao, Bing Xiao, Dacheng Tao, and Xuelong Li. A survey of graph edit distance. *Pattern Analysis and applications*, 13:113–129, 2010.
- [21] Vikas Garg, Stefanie Jegelka, and Tommi Jaakkola. Generalization and representational limits of graph neural networks. In *International Conference on Machine Learning*, pages 3419–3430. PMLR, 2020.
- [22] Justin Gilmer, Samuel S Schoenholz, Patrick F Riley, Oriol Vinyals, and George E Dahl. Neural message passing for quantum chemistry. In *International conference on machine learning*, pages 1263–1272. PMLR, 2017.
- [23] Gene H Golub and Charles F Van Loan. *Matrix computations*. JHU press, 2013.
- [24] Xiaoxue Han, Zhuo Feng, and Yue Ning. A topology-aware graph coarsening framework for continual graph learning. *arXiv preprint arXiv:2401.03077*, 2024.
- [25] Jonas MB Haslbeck and Lourens J Waldorp. How well do network models predict observations? on the importance of predictability in network models. *Behavior research methods*, 50:853–861, 2018.
- [26] David Haussler et al. Convolution kernels on discrete structures. Technical report, Citeseer, 1999.
- [27] Zhiwu Huang, Ruiping Wang, Shiguang Shan, Xianqiu Li, and Xilin Chen. Log-euclidean metric learning on symmetric positive definite manifold with application to image set classification. In *International conference on machine learning*, pages 720–729. PMLR, 2015.
- [28] Thomas N. Kipf and Max Welling. Semi-Supervised Classification with Graph Convolutional Networks. In *International Conference on Learning Representations*, 2017.
- [29] Harold W Kuhn. The hungarian method for the assignment problem. *Naval research logistics quarterly*, 2(1-2):83–97, 1955.
- [30] Tao Li, Han Dong, Yongtang Shi, and Matthias Dehmer. A comparative analysis of new graph distance measures and graph edit distance. *Information Sciences*, 403:15–21, 2017.
- [31] Jörg Liesen and Zdenek Strakos. Krylov subspace methods: principles and analysis. Numerical Mathematics and Scie, 2013.
- [32] Lek-Heng Lim, Rodolphe Sepulchre, and Ke Ye. Geometric distance between positive definite matrices of different dimensions. *IEEE Transactions on Information Theory*, 65(9):5401–5405, 2019.
- [33] Lorenzo Livi and Antonello Rizzi. The graph matching problem. *Pattern Analysis and Applications*, 16:253–283, 2013.
- [34] Andreas Loukas. Graph reduction with spectral and cut guarantees. *J. Mach. Learn. Res.*, 20(116):1–42, 2019.
- [35] Ronny Luss and Alexandre d’Aspremont. Support vector machine classification with indefinite kernels. *Advances in neural information processing systems*, 20, 2007.
- [36] Facundo Mémoli. Gromov–wasserstein distances and the metric approach to object matching. *Foundations of computational mathematics*, 11:417–487, 2011.
- [37] Christopher Morris, Martin Ritzert, Matthias Fey, William L Hamilton, Jan Eric Lenssen, Gaurav Rattan, and Martin Grohe. Weisfeiler and leman go neural: Higher-order graph neural networks. In *Proceedings of the AAAI conference on artificial intelligence*, volume 33, pages 4602–4609, 2019.
- [38] Christopher Morris, Nils M Kriege, Franka Bause, Kristian Kersting, Petra Mutzel, and Marion Neumann. Tudataset: A collection of benchmark datasets for learning with graphs. *arXiv preprint arXiv:2007.08663*, 2020.
- [39] Megan Owen and J Scott Provan. A fast algorithm for computing geodesic distances in tree space. *IEEE/ACM Transactions on Computational Biology and Bioinformatics*, 8(1):2–13, 2010.
- [40] Karl Pearson. The problem of the random walk. *Nature*, 72(1865):294–294, 1905.

- [41] Xavier Pennec, Pierre Fillard, and Nicholas Ayache. A riemannian framework for tensor computing. *International Journal of computer vision*, 66:41–66, 2006.
- [42] Jan Ramon and Thomas Gärtner. Expressivity versus efficiency of graph kernels. In *Proceedings of the first international workshop on mining graphs, trees and sequences*, pages 65–74, 2003.
- [43] Emanuele Rossi, Henry Kenlay, Maria I Gorinova, Benjamin Paul Chamberlain, Xiaowen Dong, and Michael M Bronstein. On the unreasonable effectiveness of feature propagation in learning on graphs with missing node features. In *Learning on Graphs Conference*, pages 11–1. PMLR, 2022.
- [44] Y Saad. *Numerical Methods for Large Eigenvalue Problems: Revised Edition*, volume 66. Siam, 2011.
- [45] Alberto Sanfeliu and King-Sun Fu. A distance measure between attributed relational graphs for pattern recognition. *IEEE transactions on systems, man, and cybernetics*, (3):353–362, 1983.
- [46] Gil Shamai and Ron Kimmel. Geodesic distance descriptors. In *Proceedings of the IEEE Conference on Computer Vision and Pattern Recognition*, pages 6410–6418, 2017.
- [47] Nino Shervashidze, Pascal Schweitzer, Erik Jan Van Leeuwen, Kurt Mehlhorn, and Karsten M Borgwardt. Weisfeiler-lehman graph kernels. *Journal of Machine Learning Research*, 12(9), 2011.
- [48] Daniel Spielman and ShangHua Teng. Spectral sparsification of graphs. *SIAM Journal on Computing*, 40(4):981–1025, 2011.
- [49] Vayer Titouan, Nicolas Courty, Romain Tavenard, and Rémi Flamary. Optimal transport for structured data with application on graphs. In *International Conference on Machine Learning*, pages 6275–6284. PMLR, 2019.
- [50] Matteo Togninalli, Elisabetta Ghisu, Felipe Llinares-López, Bastian Rieck, and Karsten Borgwardt. Wasserstein weisfeiler-lehman graph kernels. *Advances in neural information processing systems*, 32, 2019.
- [51] Raviteja Vemulapalli and David W Jacobs. Riemannian metric learning for symmetric positive definite matrices. *arXiv preprint arXiv:1501.02393*, 2015.
- [52] S Vichy N Vishwanathan, Nicol N Schraudolph, Risi Kondor, and Karsten M Borgwardt. Graph kernels. *The Journal of Machine Learning Research*, 11:1201–1242, 2010.
- [53] Tao Wang, He Liu, Yidong Li, Yi Jin, Xiaohui Hou, and Haibin Ling. Learning combinatorial solver for graph matching. In *Proceedings of the IEEE/CVF conference on computer vision and pattern recognition*, pages 7568–7577, 2020.
- [54] Boris Weisfeiler and Andrei Leman. The reduction of a graph to canonical form and the algebra which appears therein. *nti, Series*, 2(9):12–16, 1968.
- [55] Keyulu Xu, Weihua Hu, Jure Leskovec, and Stefanie Jegelka. How powerful are graph neural networks? In *International Conference on Learning Representations*, 2019.
- [56] Yunwen Xu, Srinivasa M Salapaka, and Carolyn L Beck. A distance metric between directed weighted graphs. In *52nd IEEE Conference on Decision and Control*, pages 6359–6364. IEEE, 2013.
- [57] Ke Ye and Lek-Heng Lim. Schubert varieties and distances between subspaces of different dimensions. *SIAM Journal on Matrix Analysis and Applications*, 37(3):1176–1197, 2016.
- [58] Kisung You and Hae-Jeong Park. Re-visiting riemannian geometry of symmetric positive definite matrices for the analysis of functional connectivity. *NeuroImage*, 225:117464, 2021.
- [59] Yuehua Zhu, Muli Yang, Cheng Deng, and Wei Liu. Fewer is more: A deep graph metric learning perspective using fewer proxies. *Advances in Neural Information Processing Systems*, 33:17792–17803, 2020.

## A Appendix

### A.1 Detailed Proofs Showing GGD is a Pseudometric

#### A.1.1 Identity Property

*Proof.* Let the corresponding SPD matrix of the graph  $G$  be  $\mathcal{L} \in \mathbb{S}_{++}^n$ . From Equation 10, we have:

$$GGD(G, G) = \left[ \sum_{i=1}^n \log^2(\lambda_i(\mathcal{L}^{-1}\mathcal{L})) \right]^{1/2} = \left[ \sum_{i=1}^n \log^2(\lambda_i(I)) \right]^{1/2}$$

The identity matrix has only one eigenvalue, which is 1. So,  $GGD(G, G) = [\log^2(1)]^{1/2} = 0$   $\square$

#### A.1.2 Positivity Property

*Proof.* Let the corresponding SPD matrices of the graphs  $G_1$  and  $G_2$  be  $\mathcal{L}_1, \mathcal{L}_2 \in \mathbb{S}_{++}^n$ . Let the generalized eigenvalues of  $(\mathcal{L}_1^{-1}\mathcal{L}_2)$  be  $\lambda_1, \lambda_2, \lambda_3, \dots, \lambda_n$ . From Equation 10, we get:

$$GGD(G_1, G_2) = [\log^2(\lambda_1) + \log^2(\lambda_2) + \log^2(\lambda_3) + \dots + \log^2(\lambda_n)]^{1/2}$$

Now,  $\log^2(\lambda_1) + \log^2(\lambda_2) + \log^2(\lambda_3) + \dots + \log^2(\lambda_n) \geq 0$ , for any values of  $\lambda_i$ .

We can conclude,  $GGD(G_1, G_2) \geq 0$ .  $\square$

#### A.1.3 Symmetry Property

*Proof.* Let the corresponding SPD matrices of the graphs  $G_1$  and  $G_2$  be  $\mathcal{L}_1, \mathcal{L}_2 \in \mathbb{S}_{++}^n$ . Let the generalized eigenvalues of  $(\mathcal{L}_1^{-1}\mathcal{L}_2)$  be  $\lambda_1, \lambda_2, \lambda_3, \dots, \lambda_n$ . From Equation 10, we get:

$$GGD(G_1, G_2) = \left[ \sum_{i=1}^n \log^2(\lambda_i) \right]^{1/2}$$

Given that the inverse of a symmetric matrix is also symmetric, and the product of two symmetric matrices is symmetric, it follows that  $(\mathcal{L}_1^{-1}\mathcal{L}_2)$  is a symmetric tensor. Furthermore, the eigenvalues of a symmetric matrix and the eigenvalues of its inverse matrix are inversely related.

So, the eigenvalues of  $(\mathcal{L}_2^{-1}\mathcal{L}_1)$  will be  $\frac{1}{\lambda_1}, \frac{1}{\lambda_2}, \frac{1}{\lambda_3}, \dots, \frac{1}{\lambda_n}$ .

$$GGD(G_2, G_1) = \left[ \sum_{i=1}^n \log^2\left(\frac{1}{\lambda_i}\right) \right]^{1/2}$$

Now,  $\log\left(\frac{1}{\lambda_i}\right) = -\log(\lambda_i)$ ; so,  $\log^2\left(\frac{1}{\lambda_i}\right) = \log^2(\lambda_i)$

So, we can conclude  $GGD(G_1, G_2) = GGD(G_2, G_1)$   $\square$

#### A.1.4 Triangle Inequality

*Proof.* Let,  $\mathcal{L}_1, \mathcal{L}_2, \mathcal{L}_3 \in \mathbb{S}_{++}^n$  are three SPD matrices corresponding to graphs  $G_1, G_2, G_3$ .

Now, The Frobenius norm  $\|X\|_F$  is the geodesic length at  $d(\exp X, I) = \|X\|_F$  [3]. Hence at identity,  $d(\mathcal{L}, I) = \|\log \mathcal{L}\|_F$ .

From [3, 58] we get,

$$GGD(G_1, G_2) = GGD\left(G_1^{-1/2}G_2G_1^{-1/2}, I\right) = \left\| \log\left(\mathcal{L}_1^{-1/2}\mathcal{L}_2\mathcal{L}_1^{-1/2}\right) \right\|_F = \left\| \log\left(\mathcal{L}_1^{-1}\mathcal{L}_2\right) \right\|_F \quad (16)$$

We know,

$$\mathcal{L}_1^{-1}\mathcal{L}_3 = \mathcal{L}_1^{-1}(\mathcal{L}_2\mathcal{L}_2^{-1})\mathcal{L}_3 = (\mathcal{L}_1^{-1}\mathcal{L}_2)(\mathcal{L}_2^{-1}\mathcal{L}_3)$$

Now using the Frobenius Norm inequality, we get:

$$\|\mathcal{L}_1^{-1}\mathcal{L}_3\| = \|(\mathcal{L}_1^{-1}\mathcal{L}_2)(\mathcal{L}_2^{-1}\mathcal{L}_3)\| \leq \|\mathcal{L}_1^{-1}\mathcal{L}_2\| \|\mathcal{L}_2^{-1}\mathcal{L}_3\|$$

Now taking logarithms on both sides:

$$\|\log(\mathcal{L}_1^{-1}\mathcal{L}_3)\| \leq \|\log(\mathcal{L}_1^{-1}\mathcal{L}_2)\| + \|\log(\mathcal{L}_2^{-1}\mathcal{L}_3)\|$$

Using Equation 10, we conclude:

$$GGD(G_1, G_3) \leq GGD(G_1, G_2) + GGD(G_2, G_3)$$

□

## A.2 Graph Matching Recovery

Given symmetric matrices  $A$ ,  $B$  and  $Z$  from the Gaussian Wigner model, where  $B_{\pi^*} = A + \sigma Z$ , there exist constants  $c, c' > 0$  such that if  $1/n^{0.1} \leq \eta \leq c/\log n$  and  $\sigma \leq c'\eta$ , then with probability at least  $1 - n^{-4}$ , GRAMPA Algorithm correctly recovers the permutation matrix  $\pi^*$ .

From 6, the similarity matrix  $\hat{X}$  is defined as:

$$\hat{X} = \sum_{i,j=1}^n \frac{u_i u_i^T \mathbf{J} v_j v_j^T}{(\zeta_i - \mu_j)^2 + \eta^2},$$

where  $u_i$  and  $v_j$  are eigenvectors of  $A$  and  $B$  respectively, and  $\zeta_i$  and  $\mu_j$  are their corresponding eigenvalues.  $\mathbf{J}$  is a all-one matrix, and  $\eta$  is the tuning parameter.

Now, the proof is divided into two parts:

**Lemma A.1** (Noiseless Setting Diagonal Dominance). *In a noiseless situation, means replacing  $B$  with  $A$ , similarity matrix  $\hat{X}^*$  is defined as:*

$$\hat{X}^* = \sum_{i,j=1}^n \frac{u_i u_i^T \mathbf{J} u_j u_j^T}{(\zeta_i - \zeta_j)^2 + \eta^2} \quad (17)$$

For some constants  $C, c > 0$ , if  $1/n^{0.1} < \eta < c/\log n$ , then with probability at least  $1 - 5n^{-5}$  for large  $n$ , it can be proved that the diagonal components of  $\hat{X}^*$  are dominant by showing [16]:

$$\min_{i \in [n]} (\hat{X}^*)_{ii} > \frac{1}{3\eta^2}, \quad \text{and} \quad \max_{i,j \in [n]: i \neq j} (\hat{X}^*)_{ij} < C \left( \frac{\sqrt{\log n}}{\eta^{3/2}} + \frac{\log n}{\eta} \right) \quad (18)$$

**Lemma A.2** (Bounding the Noise Impact). *The difference between the similarity matrix  $X$  in the presence of noise and the noiseless situation is bounded. If  $\eta > 1/n^{0.1}$ , then for a constant  $C > 0$ , with probability at least  $1 - 2n^{-5}$  for large  $n$ , it can be shown:*

$$\max_{i,j \in [n]} |\hat{X}_{ij} - (\hat{X}^*)_{ij}| < C\sigma \left( \frac{1}{\eta^3} + \frac{\log n}{\eta^2} \left( 1 + \frac{\sigma}{\eta} \right) \right) \quad (19)$$

Assuming Lemma A.1 and A.2, for some  $c, c' > 0$  sufficiently small, and by setting  $\eta < c/\log n$  and  $\sigma < c'\eta$ , the algorithm ensures that all diagonal entries of  $\hat{X}$  are larger than all off-diagonal entries, thereby achieving exact recovery.

## A.3 Effect of tuning parameter $\eta$ on Graph Matching

In the original work, it is suggested that the regularization parameter  $\eta$  needs to be chosen so that  $\sigma \vee n^{-0.1} \lesssim \eta \lesssim 1/\log n$  [16]. It is also mentioned that for practical cases, computing permutation matrix for different values of  $\eta$  in an iterative way can result in better accuracy. The GRAMPA uses  $\eta = 0.2$  for all their experiments [16].

We used a few values of  $\eta$  in the classification problem using MUTAG dataset and got that the best accuracy is obtained at  $\eta = 0.5$ . In Figure 5, the performance of the tuning parameter is demonstrated.

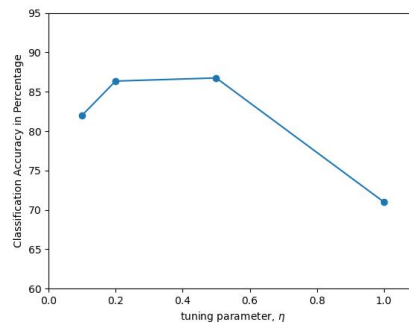


Figure 5: Classification Accuracy vs GRAMPA tuning parameter

#### A.4 Experimental Setup

To evaluate the performance of the Graph Geodesic Distance (GGD) metric, we utilized graph datasets from the TUDataset collection [38]. For small graphs, we used datasets like MUTAG and BZR, and for larger graphs, we selected PC-3H and SW-620H, which present more sizable networks.

While Classification tasks, each dataset was split into 90% training and 10% testing sets to ensure an unbiased evaluation process. When assessing the correlation with GNN, we trained a 3-layer GIN with 90% of all graphs from MUTAG and validated with the rest 10%. For the performance evaluation using graphs with partial node features, we took each dataset with node features and randomly removed a certain portion of features.

All experiments have been evaluated on a laptop with an Apple M1 chip, featuring an 8-core CPU and a 7-core GPU.